Robust Path Recommendations During Public Transit Disruptions Under Demand Uncertainty

Baichuan Mo (Corresponding Author)
PhD Candidate
Department of Civil and Environmental Engineering
Massachusetts Institute of Technology
77 Massachusetts Ave, Cambridge, MA 20139
Tel: +1 857-999-5906; Email: baichuan@mit.edu

Haris N. Koutsopoulos, Ph.D.
Professor
Department of Civil and Environmental Engineering
Northeastern University
Boston, MA 02115, United States
Tel: +1 617-373-6263; Email: h.koutsopoulos@northeastern.edu

Jinhua Zhao, Ph.D.
Associate Professor
Department of Urban Studies and Planning
Massachusetts Institute of Technology
77 Massachusetts Ave, Cambridge, MA 20139
Tel: +1 617-253-7594; Email: jinhua@mit.edu

Word count:6,952 words text + 2 table × 250 words (each) = 7,452 words

Submission Date: August 26, 2021

ABSTRACT
This paper proposes a path recommendation model to mitigate the congestion during public transit disruptions. Passengers with different origin-destinations and departure times are recommended with different paths such that the system travel time is minimized. To tackle the non-analytical formulation of travel times due to left behind, we propose a simulation-based first-order approximation to transform the original problem into linear programming. Uncertainties in demand are modeled with robust optimization techniques to protect the path recommendation strategies against inaccurate estimates. A real-world rail disruption scenario in the CTA system is used as a case study. Results show that even without considering uncertainty, the nominal model can reduce the system travel time by 9.1% (compared to status quo), and outperforms the benchmark capacity-based path recommendation. After incorporating the demand uncertainty, the robust model can further reduce the system travel time. The best robust model can decrease the average travel time of incident-line passengers by 2.91% compared to the nominal model.
Keywords: Path recommendation; Robust optimization; Stochastic optimization; Rail disruptions;

INTRODUCTION

Background

Public transit (PT) systems play an important role in urban mobility. However, with aging systems, continuous expansion, and near-capacity operations, service disruptions often occur. These incidents may result in delays, cancellation of trips, and economic losses (*1*).

During a disruption, affected passengers need to find an alternative path or use other travel modes (such as transfer to another bus route). However, due to a lack of knowledge for the system, the new routes chosen by passengers may not be optimal or even cause more congestion (*2*). For example, during a rail disruption, most of the passengers may choose some bus routes that are parallel to the interrupted rail line. However, given the limited capacity of buses, the parallel bus line may be over-saturated and passengers have to wait for a long time to board due to denied boarding (or left behind).

Objectives and Challenges

One of the strategies to better guide passengers is to provide path recommendations so that the passenger flows are re-distributed in a better way and the system travel times are reduced. This can be seen as solving an **optimal passenger flow distribution problem** over a public transit network. However, there are several challenges to this problem. First, as the objective is to reduce the system travel time, we need to have an analytical formulation to calculate passengers' travel time of a path. However, passengers' waiting time at the boarding and transfer station is not only determined by other waiting passengers, but only those who already boarded the same line as they reduce the vehicle's capacity (*3*). This complicated interaction makes it difficult to have an analytical formulation for passenger's travel time when the left behind is not negligible (which is usually the case during service disruptions). Second, there are many uncertainties in the system, such as the number of passengers that using the PT system during incidents (i.e., demand uncertainty), incident duration, and whether passengers would follow the recommendations or not (i.e., behavior uncertainty). None of the previous studies have considered uncertainties in modeling an optimal passenger flow problem.

This study aims to propose a path recommendation model to reduce the crowding during public transit disruptions and protect the recommendation results against uncertainties due to inaccurate estimates. To address the first challenge, we propose a simulation-based linearization to convert the total system travel time to a linear function of path flows using first-order approximation, which provides a tractable optimization problem. For the second challenge, this study focuses on the demand uncertainty (i.e., how many passengers will use the PT system during a service disruption) that is modeled with the robust optimization (RO) technique. The proposed approach is implemented in the Chicago Transit Authority (CTA) system with a real-world urban rail disruption as the case study.

The remainder of this paper is organized as follows. Literature review is shown in Section 2. In Section 3, we describe the problem and discuss the solution methods. We apply the proposed framework on the CTA system as a case study in Section 5. The model results are analyzed in Section 6. Finally, we conclude our study, summarize our main findings in Section 7.

LITERATURE REVIEW

Path recommendation during incidents

Most previous studies on path recommendation under incidents focus on individual or a single OD level. That is, the main objective is to find available routes or the shortest path given an OD pair when the network is interrupted by incidents. For example, Bruglieri et al. (*4*) designed a trip planner to find the fastest path in the public transit network during service disruptions based on real-time mobility information. Böhmová et al. (*5*) developed a routing algorithm in urban public transportation to find reliable journeys that are robust for system delays. Roelofsen et al. (*6*) provided a framework for generating and assessing alternatives routes in case of disruptions in urban public transport systems. To the best of the authors' knowledge, none of the previous studies have considered path recommendations at the system level, that is, providing path recommendations for passengers at different OD pairs and with different departure times so that the system travel time is reduced.

Travel time calculation in public transit networks

Passengers' travel time has two components: in-vehicle time and waiting time. In-vehicle time is not affected by passenger flows once passengers are onboard, thus is easy to model (e.g., modeled as a constant). But the waiting time is usually hard to calculate if the system is congested with left behind.

Passengers' travel time is usually modeled in the transit assignment literature, where two major frameworks exist: frequency-based (static) and schedule-based (dynamic). In the frequency-based transit assignment model, the waiting time is either assumed to be reversely proportional to the (effective) service frequency (*7–9*), or modeled as a congestion function (e.g., BRP) of previously boarded flows and new arrival flows with exogenously-calibrated parameters (*3*). The former method does not consider the left behind, and the latter method only outputs a generalized waiting cost (rather than the waiting time as the vehicle capacity is not explicitly modeled) and requires a dedicated calibration process. Therefore, the frequency-based transit assignment model is not suitable for this study because congestion and left behind are not negligible during disruptions.

In terms of the schedule-based models (*10–13*), the waiting time can only be obtained after a dynamic network loading (or simulation) process. For example, Schmöcker et al. (*13*) used the fail-to-board probability to model the left behind behavior. This probability will be updated after finishing each network loading and can be used to calculate the waiting time. However, in this way, the waiting time is still a constant within each iteration. There is no direct way to formulate waiting time as a function of path flows.

As formulating travel time as a function of path flows remains a challenge, the optimal passenger flow distribution in transit networks has no closed-form formulation. This study proposes a simulation-based first-order approximation to solve the original problem iteratively. And given a tractable linear programming model, the uncertainties can also be incorporated.

Robust optimization

RO is a common approach to handle data uncertainty in optimization problems. The general approach is to specify a range for an uncertain parameter (the "uncertainty set"), and optimize over the worst-case realizations within the bounded uncertainty set. The method is therefore well suited to applications where there is considerable uncertainty related to the model input parameters, and when data uncertainties can lead to significant penalties or infeasibility in practice. The solution method for robust optimization problems involves generating a deterministic equivalent, called the robust counterpart. Computational tractability of the robust counterpart has been a major practical difficulty (*14*). A variety of uncertainty sets have been identified for which the robust counterpart to a robust optimization problem is reasonably tractable (*15*).

The RO field has grown substantially over the past two decades. Seminal papers in the late 1990s (*16, 17*) and early 2000s (*18*) established the field. Comprehensive surveys on the early literature were done by Ben-Tal et al. (14) and Bertsimas et al. (15). The development of the robust optimization technique has allowed researchers to tackle problems with data uncertainty in a range of fields. Examples can be found for renewable energy network design (*19*), supply chain operations (*20*), health care logistics (*21*), and ride-hailing (*22*).

However, to the best of the authors' knowledge, no existing papers have incorporated robust optimization techniques into path recommendations during service disruptions. This research gap is important to address given the potential inaccurate estimates of demand in public transit networks during an incident.

METHODOLOGY

Problem description

Consider a service disruption in an urban rail system start at time T_s and end at T_e. During the disruption, some stations in the incident line (or the whole line) are blocked. Passengers in the blocked trains are usually offloaded to the nearest platforms. To respond to the incident, some operation changes are made, such as dispatching shuttle buses, rerouting existing services, short-turning in the incident line, headway adjustment, etc. Assume that we have all information about the operation changes. These changes define a new PT service network and available path sets. Our objective is to design an origin-destination (OD) based recommendation system. That is, when the incident happens, passengers can use their phones, websites, or electrical boards at stations to access the system, inputting their **origin, destination, and departure time** to get a recommended path. And the recommendation aims to minimize the system travel time, that is, the sum of all passengers' travel time, including passengers in nearby lines or bus routes without incidents (note that these passengers may experience additional crowding due to transfer passengers from the incident line).

Let $\mathcal{K}$ be the pre-determined set of all Od pairs that may need path recommendation. $\mathcal{K}$ is defined based on whether passengers with the OD are affected by the incident or not. Note that as the path recommendation starts at T_s, the origin for passengers who are already in the system (e.g., offloaded passengers from the blocked vehicles) is their current location (as opposed to their initial origin such as the boarding station). We aim to provide recommendations for passengers whose OD pair in $\mathcal{K}$ and departure time in the range from T_s to some time after T_e, because the congestion may last longer than T_e, passengers depart after T_e may also need guidance. We divide the periods of recommendation into a time point (h_0) and several equal-length time intervals ($h_1,...,h_H$). Specifically, h_0 represent the time point at T_s. Recommendations at T_s focus on passengers who are already in the system (and their departure times are T_s). And h_t ($t \geq 1$) represents the time interval $(T_s + (t-1)\tau, T_s + t\tau]$, where τ is the length of a time interval (e.g., 10 min). Recommendations at h_t ($t \geq 1$) focus on passengers who have not entered the system when the incident happens and their departure times are in $(T_s + (t-1)\tau, T_s + t\tau]$. Let the set of all recommendation times be $\mathcal{H} := \{h_0, h_1, ..., h_H\}$.

Given the new operation after T_s, we can obtain a feasible path set R_k for each OD pair k. Note that R_k includes all feasible services that are provided by the PT operator. A path $r \in R_k$ may be waiting for the system to recover (i.e., using the incident line), or transfer to nearby bus lines, using shuttle services, etc. We do not consider non-PT modes such as Uber or driving for the following reasons: 1) This study aims to design a path recommendation system used by PT operators. The major audience should be all PT users. Considering non-PT modes needs the supply information of all other travel modes and even consider non-PT users (such as the impact of traffic congestion on drivers), which is beyond the scope of this study. Future research may consider a multi-modal path recommendation system. 2) Passengers using non-PT modes can be simply treated as demand reduction for the PT system. So their impact on the PT system is still captured.

Let d_{hk} be the number of passengers using PT system with OD pair $k \in \mathcal{K}$ and departure time $h \in \mathcal{H}$. It can be treated as the normal demand minus the number of passengers leaving the PT system. As we do not have full information about future demand and number of passengers leaving the system, d_{hk} is an uncertainty variable which will be discussed in Section 3.4. Let f_{hkr} be the number of passengers departing at time interval h, with OD pair k, and using path $r \in R_k$. By definition:

$$\sum_{r \in R_k} f_{hkr} = d_{hk} \quad \forall h \in \mathcal{H}, k \in \mathcal{K} \tag{1}$$

Let p_{hkr} be the corresponding path share of f_{hkr} (i.e., $p_{hkr} = f_{hkr}/d_{hk}$ and $\sum_{r \in R_k} p_{hkr} = 1$). For the convenience of description, we define $\mathcal{F} := \{(h,k,r) : \forall h \in \mathcal{H}, \forall k \in \mathcal{K}, r \in R_k\}$ as a set of all path indices. Then the optimal flow problem can be formulated as:

$$\min_{\boldsymbol{f},\boldsymbol{p}} \quad Z(\boldsymbol{f}) = \text{Sum of all passengers' travel time} \tag{2a}$$

$$\text{s.t.} \quad \sum_{r \in R_k} p_{hkr} = 1 \qquad \forall\, h \in \mathcal{H}, k \in \mathcal{K}, \tag{2b}$$

$$f_{hkr} = d_{hk} \cdot p_{hkr} \quad \forall\, (h,k,r) \in \mathcal{F}, \tag{2c}$$

$$f_{hkr} \geq 0 \qquad \forall\, (h,k,r) \in \mathcal{F}, \tag{2d}$$

$$0 \leq p_{hkr} \leq 1 \qquad \forall\, (h,k,r) \in \mathcal{F} \tag{2e}$$

where $\boldsymbol{f} := (f_{hkr})_{h,k,r \in \mathcal{F}}$ and $\boldsymbol{p} := (p_{hkr})_{h,k,r \in \mathcal{F}}$. $Z(\boldsymbol{f})$ is the system travel time which has no analytical expression. It can only be obtained after each network loading or simulation process (see Section 2.2). Note that using both of $\boldsymbol{f}$ and $\boldsymbol{p}$ in the optimization problem is redundant, but it is useful for the methodology explanation.

If there was no uncertainty in the system and all passengers follow the recommendation, the optimal path shares (p^*_{hkr}) solved from Eq. 2 are the recommendation proportion. That is, for all passengers who input OD pair k and departure time h, the system will recommend them to use path r with probability p^*_{hkr}. However, Eq. 2 is just a naive formulation. We cannot solve it directly because $Z(\boldsymbol{f})$ has no analytical expression. Moreover, given the uncertainties in demand, the final recommended path shares may not be p^*_{hkr}. In the following section, we elaborate on how to solve the "optimal flow problem" with demand uncertainties.

Event-based public transit simulator

Before introducing the solution procedure for Eq. 2, we first describe an event-based public transit simulator used in this study (*23*). It can be used to evaluate $Z(f)$ and facilitate the simulation-based linearization.

Figure 1 summarizes the main structure of the simulator. The inputs for the simulator are time-dependent OD demand (or smart card data), path shares, network structure, and train movement data (or timetable). Three objects are defined: trains, queues, and passengers. Trains are characterized by routes, runs, current locations, and capacities. Passengers are queued based on their arrival times. Three different types of passengers are represented: left-behind passengers who were denied boarding from previous trains, new tap-in passengers from outside the system, and new transfer passengers from other lines. The left-behind passengers are usually at the head of the queue.

An event-based modeling framework is used to load the passengers onto the network. Two types of events are considered: train arrivals and train departures. The events are sorted by time and processed sequentially until all events are successfully completed during the analysis period. Train event lists (arrivals and departures) are generated according to the actual train movement data or timetable. Each event contains a train ID, occurrence time, and location (platform). Passengers are assigned to a path based on the corresponding input path shares. Note that in this study, a "path" is defined with specific boarding and transfer stations and lines. Two journeys that share a common line can be treated as two different paths. Hence, there is no "common line" problem (*3*) in this study.

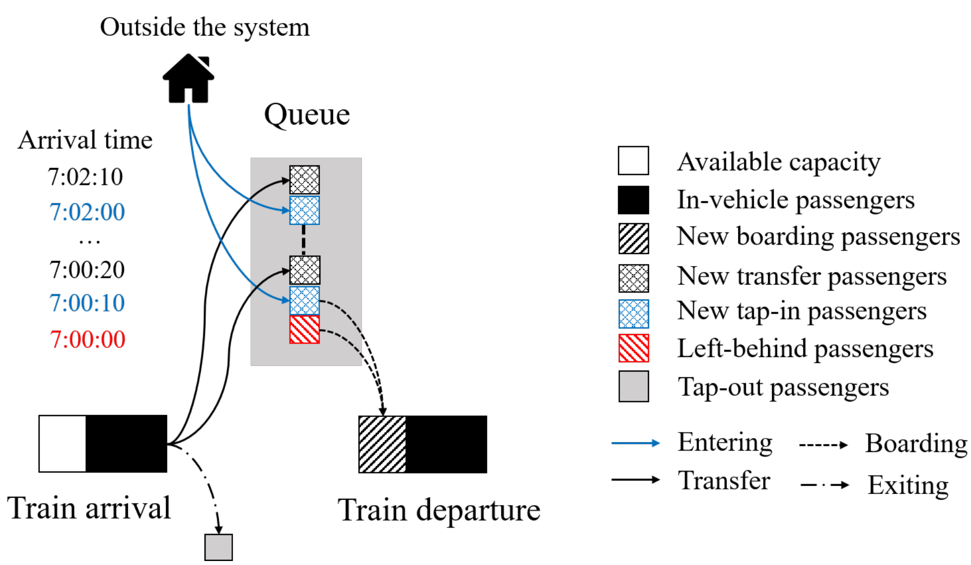

FIGURE 1: Structure of the network loading model

For an arrival event, the train offloads passengers who reach their destination or need to transfer at the station and updates its state (e.g. train load and in-vehicle passengers). For passengers who reach their destinations, their tap-out times are calculated by adding their egress time. For those who transfer at the station, their arrival times at the next platform are calculated based on the transfer time. The transfer passengers are added to the waiting queue in order of their arrival times at the next platform.

For departure events, the queue on the platform is updated by the new tap-in passengers, that is, passengers who arrive at the platform after the last train departed are added into the queue based on their arrival times. Passengers board the train according to a First-Come-First-Serve (FCFS) discipline until the train reaches its capacity. Passengers who cannot board are left behind and wait in the queue for the next train. The states of the train and the waiting queue are updated accordingly.

The simulator can record every passenger's trajectory during the whole travel process, including tap-in time, platform arrival time, boarding time, alighting time, tap-out time, etc. This information can be used for the simulation-based linearization of the objective function $Z(\boldsymbol{f})$.

Simulation-based linearization of the objective function

In this section, we propose a simulation-based linearization for the non-analytical $Z(\boldsymbol{f})$ based on the first-order approximation. Notice that $Z(\boldsymbol{f})$ can be approximated as:

$$\hat{Z}(\boldsymbol{f}) = Z(\tilde{\boldsymbol{f}}) + (\boldsymbol{f} - \tilde{\boldsymbol{f}})^T \frac{\partial Z(\boldsymbol{f})}{\partial \boldsymbol{f}}|_{\boldsymbol{f}=\tilde{\boldsymbol{f}}} \tag{3}$$

where $\hat{Z}(\boldsymbol{f})$ is the first-order approximation of $Z(\boldsymbol{f})$. $\tilde{\boldsymbol{f}}$ is a reference flow for the first-order approximation. $Z(\tilde{\boldsymbol{f}})$ is the system travel time estimated by simulation with $\tilde{\boldsymbol{f}}$ as inputs. $\frac{\partial Z(f)}{\partial f} = (\frac{\partial Z(f)}{\partial f_{hkr}})_{h,k,r\in\mathcal{F}}$ is the gradient vector of $Z(\boldsymbol{f})$. As $\tilde{\boldsymbol{f}}$ and $Z(\tilde{\boldsymbol{f}})$ are pre-determined, the only unknown part is $\frac{\partial Z(f)}{\partial f}|_{f=\tilde{f}}$. Notice that $\frac{\partial Z(f)}{\partial f_{hkr}}|_{f=\tilde{f}}$ represents the change of system travel time caused by one unit of flow change in f_{hkr}, it can be approximated as:

$$\frac{\partial Z(\boldsymbol{f})}{\partial f_{hkr}}|_{f=\tilde{f}} \approx \frac{Z(\tilde{\boldsymbol{f}} + \boldsymbol{e}_{hkr}) - Z(\tilde{\boldsymbol{f}})}{1} \tag{4}$$

where $\boldsymbol{e}_{hkr}$ represents a vector with only the (h,k,r)-th element being 1 and others being zero. Eq. 4 represents the numerical approximation of the gradient. Then we only need to calculate $Z(\tilde{\boldsymbol{f}} + \boldsymbol{e}_{hkr}) - Z(\tilde{\boldsymbol{f}})$. One of the naive method to is to run a simulation with $\tilde{\boldsymbol{f}} + \boldsymbol{e}_{hkr}$ as input. However, as running the simulation is time-consuming, this method is not efficient. Since we already run a simulation for $\tilde{\boldsymbol{f}}$, it is possible to directly calculate the marginal change without running it again. Given the definition of the gradient, the problem is to calculate the additional travel time increase to the system if one additional flow is added to $\tilde{f}_{hkr}$.

Consider an example journey of $\tilde{f}_{hkr}$ in Figure 2. Let M_{hkr} be the set of passengers that counting the flow of $\tilde{f}_{hkr}$ (i.e., the orange one in Figure 2). These passengers have origin of station a_1 and destination of station a_7, and the path includes a transfer from station a_4 to station a_5. Denote the average travel time of $\tilde{f}_{hkr}$ as $T^{\text{A}}_{hkr}(\tilde{\boldsymbol{f}})$. Suppose that we want to add one more passenger to $\tilde{f}_{hkr}$ (i.e., the orange passenger is duplicated in Figure 2). First of all, the system travel time is increased by $T^{\text{A}}_{hkr}(\tilde{\boldsymbol{f}})$ due to the increase in the flow amount.

Besides, it may also affect other passengers' travel time. All passengers in the red-dashed square may be affected. Passengers at station a_1 and a_5 who queue behind the orange passenger may have additional waiting time if the vehicle that M_{hkr} used is full after departure (under the simulation results of $\tilde{\boldsymbol{f}}$), because the increase of one flow in $\tilde{f}_{hkr}$ will occupy the one capacity for these waiting passengers, and one of them have to board the next bus (i.e., wait for one more

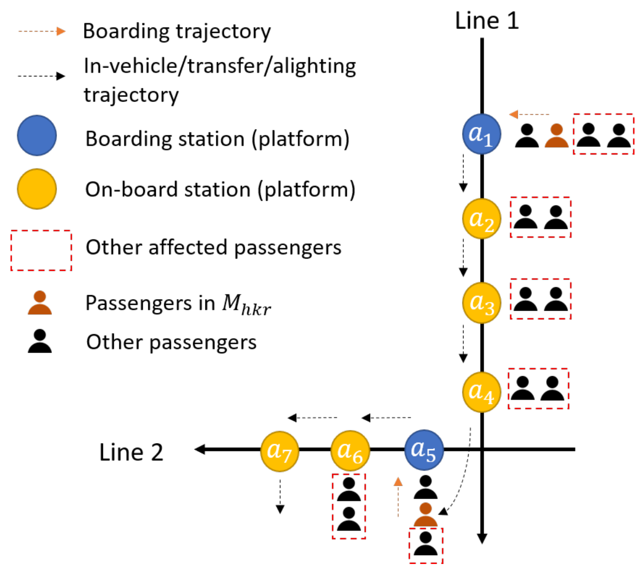

FIGURE 2: Explanation for the impact of adding additional one unit flow to the system

headway). Mathematically, let V^b_{hkr} be the set of vehicles that M_{hkr} board at station b, adding an additional passenger to M_{hkr} means we have one more passenger board in one of the vehicles in V^b_{hkr}. Let $\mathbb{1}_{\{\text{Full}^b_v\}}$ be an indicator of whether vehicle v is full or not after departure from station b, then the total increase in system travel time for passengers queuing behind M_{hkr} is:

$$T^{\text{Q}}_{hkr}(\tilde{f}) = \sum_{b \in B_{hkr}} \sum_{v \in V^b_{hkr}} \frac{\mathbb{1}_{\{\text{Full}^b_v\}} \cdot H^b_v}{|V^b_{hkr}|} \tag{5}$$

where B_{hkr} is the set of all boarding stations of M_{hkr} (in this example, a_1 and a_5). H^b_v is the headway of vehicle v at station b. The sum over all vehicles is because we do not specify the exact vehicle that the additional passenger will board, and thus take the average over all vehicles. In this example, since there are two boarding stations for M_{hkr} (a_1, a_5), the total travel time increases are around two headways if the vehicles are full.

For passengers waiting at stations where M_{hkr} are on-board (referred to as on-board stations, e.g., station a_2), adding one flow to $\tilde{f}_{hkr}$ reduces the available capacity when the vehicle arrives at the on-board stations. And the queuing passengers at the on-board stations may not be able to board due to the reduction of capacity. Specifically, if a vehicle is full when it departs from an onboard station under flow pattern $\tilde{f}$, adding one flow to $\tilde{f}_{hkr}$ makes one passenger waiting at the on-board station unable to board his/her original boarded vehicle. And the system travel time is increased by one headway for each of these onboard stations. Mathematically, let O^v_{hkr} be the set of all on-board stations for M_{hkr} and vehicle $v \in V^b_{hkr}$. For example, for vehicles in Line 1, O^v_{hkr} will be a_2, a_3, and a_4. Then the travel time increase for passengers waiting at on-board stations is:

$$T^{\text{O}}_{hkr}(\tilde{f}) = \sum_{b \in B_{hkr}} \sum_{v \in V^b_{hkr}} \frac{1}{|V^b_{hkr}|} \sum_{a \in O^v_{hkr}} \mathbb{1}_{\{\text{Full}^a_v\}} \cdot H^a_v \tag{6}$$

Therefore, in this way, depending on whether the vehicle is full or not under flow pattern $\tilde{\boldsymbol{f}}$, we can calculate the increase in system travel time due to adding one flow to $\tilde{f}_{hkr}$ without running the simulation again. These increases come from three parts: 1) the average travel time of M_{hkr} due to increasing in flow amount, 2) the additional waiting time for passengers queuing behind M_{hkr}, and 3) the additional waiting time for passengers queuing at M_{hkr}'s on-board stations. Specifically, we have

$$Z(\tilde{\boldsymbol{f}} + \boldsymbol{e}_{hkr}) - Z(\tilde{\boldsymbol{f}}) = T^{\mathrm{A}}_{hkr}(\tilde{\boldsymbol{f}}) + T^{\mathrm{Q}}_{hkr}(\tilde{\boldsymbol{f}}) + T^{\mathrm{O}}_{hkr}(\tilde{\boldsymbol{f}}) \tag{7}$$

Consequently, $\frac{\partial Z(f)}{\partial f}|_{f=\tilde{f}}$ can be obtained from Eq. 4. Define $\boldsymbol{\beta}(\tilde{\boldsymbol{f}}) := \frac{\partial Z(f)}{\partial f}|_{f=\tilde{f}}$. Then the objective function becomes:

$$\hat{Z}(\boldsymbol{f}) = Z(\tilde{\boldsymbol{f}}) + \boldsymbol{\beta}(\tilde{\boldsymbol{f}})^T(\boldsymbol{f} - \tilde{\boldsymbol{f}}) \tag{8}$$

where $\boldsymbol{\beta}(\tilde{\boldsymbol{f}}) = (\beta_{hkr})_{h,k,r\in\mathcal{F}}$ and $\beta_{hkr} = \frac{\partial Z(f)}{\partial f_{hkr}}|_{f=\tilde{f}}$. Eq. 8 is a linear function of $\boldsymbol{f}$, which supports for addressing uncertainties in the optimization problem.

Demand uncertainty

The uncertainty of d_{hk} comes from two different parts. The first is the inherent demand variations across different days, and the second is the uncertainty in how many passengers leaving the PT system during the incident. In this section, these two parts of uncertainties are considered as a whole by introducing an ellipsoidal uncertainty set and two polyhedral uncertainty sets.

From the constraint 2c, we can substitute $f_{hkr} = d_{hk} \cdot p_{hkr}$ to the objective function and rewriting Eq. 8 as:

$$\hat{Z}(\boldsymbol{f}) = \hat{Z}(\boldsymbol{p}) = Z(\tilde{\boldsymbol{f}}) + \sum_{(h,k,r)\in\mathcal{F}} \beta_{hkr} \cdot (d_{hk} \cdot p_{hkr} - \tilde{f}_{hkr}) \tag{9}$$

Note that β_{hkr} is a function of $\tilde{\boldsymbol{f}}$, for simplicity we ignore it in the derivation process.

To model the uncertainty of d_{hk}, we introduce an auxiliary decision variable t and rewrite the optimal flow problem as:

$$\min_{\boldsymbol{p},t} \quad t \tag{10a}$$

$$\text{s.t.} \quad t \geq Z(\tilde{\boldsymbol{f}}) + \sum_{(h,k,r)\in\mathcal{F}} \beta_{hkr} \cdot (d_{hk} \cdot p_{hkr} - \tilde{f}_{hkr}), \tag{10b}$$

$$\text{Other constraints omitted} \tag{10c}$$

Constraint 10b can be rewritten as

$$\sum_{h,k} \sum_{r\in R_k} \beta_{hkr} \cdot d_{hk} \cdot p_{hkr} \leq t - Z(\tilde{\boldsymbol{f}}) + \sum_{(h,k,r)\in\mathcal{F}} \beta_{hkr} \tilde{f}_{hkr} \tag{11}$$

And Eq. 11 can be written as a matrix form:

$$\boldsymbol{a}^T\boldsymbol{p} \le b \tag{12}$$

where $\boldsymbol{a} \in \mathbb{R}^{|\mathcal{F}|}$ with the entry $a_{hkr} = \beta_{hkr} d_{hk}$, $\forall\,(h,k,r) \in \mathcal{F}$. And $b = t - Z(\tilde{\boldsymbol{f}}) + \sum_{(h,k,r)\in\mathcal{F}} \beta_{hkr}\tilde{f}_{hkr}$. Define $\boldsymbol{d} = (d_{hk})_{h\in\mathcal{H},k\in\mathcal{K}}$.

Proposition 1. If $\boldsymbol{d}$ is normally distributed with $\boldsymbol{d} \sim \mathcal{N}(\bar{\boldsymbol{d}}, \boldsymbol{\Sigma})$, then in a RO problem where constraint 12 is guaranteed to be satisfied with probability of at least $1-\varepsilon$ (i.e., $\mathbb{P}[\boldsymbol{a}^T\boldsymbol{p} \le b] \ge 1-\varepsilon$), the robust constraint can be formulated as:

$$(\boldsymbol{A}\bar{\boldsymbol{d}} + \boldsymbol{A}\boldsymbol{D}\boldsymbol{z})^T\boldsymbol{p} \le b, \quad \forall \boldsymbol{z} \in \mathcal{Z}_{\mathrm{E}} \tag{13}$$

where $\boldsymbol{A} \in \mathbb{R}^{|\mathcal{F}|\times HK}$ and the entry is defined as $A_{hkr,h'k'} = \beta_{hkr}$ if $h = h'$ and $k = k'$, otherwise $A_{hkr,h'k'} = 0$. $\boldsymbol{D}$ is the Cholesky decomposition of $\boldsymbol{\Sigma}$ (i.e., $\boldsymbol{\Sigma} = \boldsymbol{D}\boldsymbol{D}^T$). $\boldsymbol{z}$ is the perturbation variables (i.e., $\boldsymbol{d} = \bar{\boldsymbol{d}} + \boldsymbol{D}\boldsymbol{z}$) and $\mathcal{Z}_{\mathrm{E}} = \left\{\boldsymbol{z} \in \mathbb{R}^{HK} : \|z\|_2 \le \rho_{1-\varepsilon}\right\}$ (i.e., the ellipsoidal uncertainty set). $\rho_{1-\varepsilon}$ is the $(1-\varepsilon)$-percentile of a standard normal distribution.

Proof. **Step 1:** We first prove that $\mathbb{P}[\boldsymbol{a}^T\boldsymbol{p} \le b] \ge 1-\varepsilon$ is equivalent to $(\boldsymbol{A}\bar{\boldsymbol{d}})^T\boldsymbol{p} + \rho_{1-\varepsilon}\left\|(\boldsymbol{A}\boldsymbol{D})^T\boldsymbol{p}\right\|_2 \le b$.

Since $\boldsymbol{d}$ is normally distributed, we have $\boldsymbol{a} = \boldsymbol{A}\boldsymbol{d}$ is normally distributed with $\boldsymbol{a} \sim \mathcal{N}(\boldsymbol{A}\bar{\boldsymbol{d}}, \boldsymbol{A}\Sigma\boldsymbol{A}^T)$. Similarly, $\boldsymbol{a}^T\boldsymbol{p} \in \mathbb{R}$ is also normally distributed with

$$\boldsymbol{a}^T\boldsymbol{p} \sim \mathcal{N}((\boldsymbol{A}\bar{\boldsymbol{d}})^T\boldsymbol{p}, \boldsymbol{p}^T\boldsymbol{A}\boldsymbol{\Sigma}\boldsymbol{A}^T\boldsymbol{p}) \tag{14}$$

If we want constraint 12 to hold with probability at least $1-\varepsilon$, it suffices to have:

$$(\boldsymbol{A}\bar{\boldsymbol{d}})^T\boldsymbol{p} + \rho_{1-\varepsilon}\sqrt{\boldsymbol{p}^T\boldsymbol{A}\boldsymbol{\Sigma}\boldsymbol{A}^T\boldsymbol{p}} \le b \tag{15}$$

Substituting $\boldsymbol{\Sigma} = \boldsymbol{D}\boldsymbol{D}^T$ into Eq. 15 finishes the proof of Step 1.

Step 2: We need to show that the robust counterpart of Eq. 13 is $(\boldsymbol{A}\bar{\boldsymbol{d}})^T\boldsymbol{p} + \rho_{1-\varepsilon}\left\|(\boldsymbol{A}\boldsymbol{D})^T\boldsymbol{p}\right\|_2 \le b$.

Notice that Eq. 13 is equivalent to:

$$(\boldsymbol{A}\bar{\boldsymbol{d}})^T\boldsymbol{p} + \max_{\boldsymbol{z}\in\mathcal{Z}_{\mathrm{E}}}(\boldsymbol{A}\boldsymbol{D}\boldsymbol{z})^T\boldsymbol{p} \le b. \tag{16}$$

Define the indicator function on set $\mathcal{Z}_{\mathrm{E}}$ as

$$\delta(\boldsymbol{z} \mid \mathcal{Z}_{\mathrm{E}}) = \begin{cases} 1, & \text{if } \boldsymbol{z} \in \mathcal{Z}_{\mathrm{E}} \\ 0, & \text{otherwise} \end{cases} \tag{17}$$

Then the convex conjugate of $\delta(\boldsymbol{z} \mid \mathcal{Z}_{\mathrm{E}})$ (also known as the **support function**) can be derived as (*24*):

$$\delta^*(\boldsymbol{y} \mid \mathcal{Z}_{\mathrm{E}}) = \sup_{\boldsymbol{z}\in\mathbb{R}^{HK}}\{\boldsymbol{y}^T\boldsymbol{z} - \delta(\boldsymbol{z} \mid \mathcal{Z}_{\mathrm{E}})\} = \sup_{\boldsymbol{z}\in\mathcal{Z}_{\mathrm{E}}} \boldsymbol{y}^T\boldsymbol{z} = \rho_{1-\varepsilon}\|\boldsymbol{y}\|_2 \tag{18}$$

Therefore, Eq. 16 can be rewritten with the convex conjugate:

$$(\boldsymbol{A}\bar{\boldsymbol{d}})^T\boldsymbol{p} + \delta^*((\boldsymbol{A}\boldsymbol{D})^T\boldsymbol{p} \mid \mathcal{Z}) = (\boldsymbol{A}\bar{\boldsymbol{d}})^T\boldsymbol{p} + \rho_{1-\varepsilon}\left\|(\boldsymbol{A}\boldsymbol{D})^T\boldsymbol{p}\right\|_2 \le b \tag{19}$$

which finishes the proof of Step 2. Combining step 1 and 2 finishes the proof of the whole proposition. □

Remark 1. In the RO, the ellipsoidal uncertainty set can be used no matter what distribution $\boldsymbol{d}$ follows. If $\boldsymbol{d}$ is normally distributed, the parameter $\rho_{1-\varepsilon}$ could have a specific meaning and we can characterize the probability for that constraint 12 holds. The use of multivariate normality assumption in Proposition 1 is for explaining the physical meaning of ellipsoidal uncertainty set and facilitating the choice of hyperparameters (i.e., $\rho_{1-\varepsilon}$ and $\boldsymbol{D}$). Moreover, in the case study, we partially validate the multivariate normality assumption of $\boldsymbol{d}$ using smart card data. The Mardia's Skewness Test (*25*) shows that $\boldsymbol{d}$ has no significant skewness.

Eq. 13 (i.e., the ellipsoidal uncertainty set) captures the correlation between demands at different time intervals and OD pairs. However, it does not impose any upper or lower bounds to d_{hk}. In reality, the demand level for a specific OD pair and time interval is usually bounded, which can be expressed as:

$$d_{hk}^{\mathrm{L}} \le d_{hk} \le d_{hk}^{\mathrm{U}} \tag{20}$$

where d_{hk}^{L} and d_{hk}^{U} are the corresponding lower and upper bounds for d_{hk}, respectively. Their values can be obtained from historical demand data. Eq. 20 can be rewritten in a vector form as $\boldsymbol{d}^{\mathrm{L}} \le \boldsymbol{d} \le \boldsymbol{d}^{\mathrm{U}}$, where $\boldsymbol{d}^{\mathrm{U}} = (d_{hk}^{\mathrm{U}})_{h\in\mathcal{H},k\in\mathcal{K}}$ and $\boldsymbol{d}^{\mathrm{L}} = (d_{hk}^{\mathrm{L}})_{h\in\mathcal{H},k\in\mathcal{K}}$. Since we have $\boldsymbol{d} = \bar{\boldsymbol{d}} + \boldsymbol{D}\boldsymbol{z}$, a simple manipulation leads to

$$\boldsymbol{d}^{\mathrm{L}} - \bar{\boldsymbol{d}} \le \boldsymbol{D}\boldsymbol{z} \le \boldsymbol{d}^{\mathrm{U}} - \bar{\boldsymbol{d}} \tag{21}$$

We can rewritten it as a "polyhedral uncertainty set": $\mathcal{Z}_{\mathrm{P1}} = \left\{\boldsymbol{z} \in \mathbb{R}^{HK} : \boldsymbol{d}^{\mathrm{L}} - \bar{\boldsymbol{d}} \le \boldsymbol{D}\boldsymbol{z} \le \boldsymbol{d}^{\mathrm{U}} - \bar{\boldsymbol{d}}\right\}$.

Eq. 20 ensures the boundaries for each individual demand. Another similar constraint for the demand uncertainty is that: within a given time interval, the total demand across all OD pairs should also be bounded. This constraint can avoid some extreme scenarios that Eq. 20 cannot capture (e.g., all d_{hk} are at the lower or upper bounds). Mathematically:

$$d_h^{\mathrm{L}} \le \sum_{k\in\mathcal{K}} d_{hk} \le d_h^{\mathrm{U}} \tag{22}$$

where d_h^{L} and d_h^{U} are the lower and upper bounds for the total demand in time interval h, which can be obtained from the historical demand. Define $\boldsymbol{S} \in \mathbb{R}^{H\times HK}$, where the element $S_{h,h'k} = 1$ if $h = h'$, otherwise $S_{h,h'k} = 0$. Then Eq. 22 can be rewritten in a matrix form:

$$\boldsymbol{d}_{\mathcal{H}}^{\mathrm{L}} - \boldsymbol{S}\bar{\boldsymbol{d}} \le \boldsymbol{S}\boldsymbol{D}\boldsymbol{z} \le \boldsymbol{d}_{\mathcal{H}}^{\mathrm{U}} - \boldsymbol{S}\bar{\boldsymbol{d}} \tag{23}$$

where $\boldsymbol{d}_{\mathcal{H}}^{\mathrm{U}} = (d_h^{\mathrm{U}})_{h\in\mathcal{H}}$ and $\boldsymbol{d}_{\mathcal{H}}^{\mathrm{L}} = (d_h^{\mathrm{L}})_{h\in\mathcal{H}}$. And Eq. 23 can also be represented as a polyhedral uncertainty set: $\mathcal{Z}_{\mathrm{P2}} = \left\{ \boldsymbol{z} \in \mathbb{R}^{HK} : \boldsymbol{d}_{\mathcal{H}}^{\mathrm{L}} - \boldsymbol{S}\bar{\boldsymbol{d}} \leq \boldsymbol{S}\boldsymbol{D}\boldsymbol{z} \leq \boldsymbol{d}_{\mathcal{H}}^{\mathrm{U}} - \boldsymbol{S}\bar{\boldsymbol{d}} \right\}$.

Therefore, the final robust constraint for Eq. 12 is

$$(\boldsymbol{A}\bar{\boldsymbol{d}} + \boldsymbol{A}\boldsymbol{D}\boldsymbol{z})^T \boldsymbol{p} \leq b, \quad \forall \boldsymbol{z} \in \mathcal{Z}_{\mathrm{E}} \cap \mathcal{Z}_{\mathrm{P1}} \cap \mathcal{Z}_{\mathrm{P2}} \tag{24}$$

To derive the robust counterpart of the constraint, we first introduce the following lemma.

Lemma 1. For a constraint $\bar{\boldsymbol{a}}^T \boldsymbol{x} + \delta^*(\boldsymbol{P}^T \boldsymbol{x} \mid \mathcal{Z}) \leq b$, let $\mathcal{Z}_1, \ldots, \mathcal{Z}_k$ be closed convex sets, such that $\bigcap_i ri(\mathcal{Z}_i) \neq \emptyset$[1], and let $\mathcal{Z} = \cap_{i=1}^k \mathcal{Z}_i$. Then,

$$\delta^*(\boldsymbol{y} \mid \mathcal{Z}) = \min_{\boldsymbol{y}_1, \ldots, \boldsymbol{y}_k} \{ \sum_{i=1}^k \delta^*(\boldsymbol{y}_i \mid \mathcal{Z}_i) \mid \sum_{i=1}^k \boldsymbol{y}_i = \boldsymbol{y} \},$$

and the constraint becomes

$$\begin{cases} \bar{\boldsymbol{a}}^T \boldsymbol{x} + \sum_{i=1}^k \delta^*(\boldsymbol{y}_i \mid \mathcal{Z}_i) \leq b \\ \sum_{i=1}^k \boldsymbol{y}_i = \boldsymbol{P}^T \boldsymbol{x} \end{cases}$$

where $\delta^*(\cdot \mid \cdot)$ is the support function (i.e., convex conjugate of the indicator function).

From Proposition 1, we have $\delta^*(\boldsymbol{y} \mid \mathcal{Z}_{\mathrm{E}}) = \rho_{1-\varepsilon} \|\boldsymbol{y}\|_2$. For the polyhedral uncertainty set, consider a general form $\mathcal{Z}_{\mathrm{P}} = \{\boldsymbol{z} : \boldsymbol{H}\boldsymbol{z} \leq \boldsymbol{c}\}$. And the support function for $\mathcal{Z}_{\mathrm{P}}$ is

$$\delta^*(\boldsymbol{y} \mid \mathcal{Z}_{\mathrm{P}}) = \max_{\boldsymbol{z}} \{\boldsymbol{y}^T \boldsymbol{z} \mid \boldsymbol{H}\boldsymbol{z} \leq \boldsymbol{c}\} = \min_{\boldsymbol{u}} \{\boldsymbol{c}^T \boldsymbol{u} \mid \boldsymbol{H}^T \boldsymbol{u} = \boldsymbol{y}, \boldsymbol{u} \geq 0\} \tag{25}$$

where the second equality follows from linear programming duality. Eq. 25 can be used to derive the support function for $\mathcal{Z}_{\mathrm{P}}$. Based on Lemma 1, the robust counterpart for Eq. 24 is

$$\begin{cases} (\boldsymbol{A}\bar{\boldsymbol{d}})^T \boldsymbol{p} + \rho_{1-\varepsilon} \|\boldsymbol{y}_1\|_2 + (\boldsymbol{d}^{\mathrm{U}} - \bar{\boldsymbol{d}})^T \boldsymbol{u}_1 + (\bar{\boldsymbol{d}} - \boldsymbol{d}^{\mathrm{L}})^T \boldsymbol{u}_2 + (\boldsymbol{d}_{\mathcal{H}}^{\mathrm{U}} - \boldsymbol{S}\bar{\boldsymbol{d}})^T \boldsymbol{v}_1 + (\boldsymbol{S}\bar{\boldsymbol{d}} - \boldsymbol{d}_{\mathcal{H}}^{\mathrm{L}})^T \boldsymbol{v}_2 \leq b \\ \boldsymbol{D}^T \boldsymbol{u}_1 = \boldsymbol{y}_2 \\ -\boldsymbol{D}^T \boldsymbol{u}_2 = \boldsymbol{y}_3 \\ (\boldsymbol{S}\boldsymbol{D})^T \boldsymbol{v}_1 = \boldsymbol{y}_4 \\ -(\boldsymbol{S}\boldsymbol{D})^T \boldsymbol{v}_2 = \boldsymbol{y}_5 \\ \sum_{i=1}^5 \boldsymbol{y}_i = (\boldsymbol{A}\boldsymbol{D})^T \boldsymbol{p} \\ \boldsymbol{u}_1, \boldsymbol{u}_2, \boldsymbol{v}_1, \boldsymbol{v}_2 \geq 0 \end{cases} \tag{26}$$

[1] $ri(\mathcal{Z}_i)$ indicates the relative interior of the set $\mathcal{Z}_i$.

Hence, the RO can be formulated as

$$\min_{\boldsymbol{p},\boldsymbol{u},\boldsymbol{v},\boldsymbol{y},t} \quad t \tag{27a}$$

$$\text{s.t.} \quad \sum_{(h,k,r)\in\mathcal{F}} \beta_{hkr} \cdot d_{hk} \cdot p_{hkr} + \rho_{1-\varepsilon} \|\boldsymbol{y}_1\|_2 + (\boldsymbol{d}^{\mathrm{U}} - \bar{\boldsymbol{d}})^T \boldsymbol{u}_1 + (\bar{\boldsymbol{d}} - \boldsymbol{d}^{\mathrm{L}})^T \boldsymbol{u}_2$$
$$+ (\boldsymbol{d}^{\mathrm{U}}_{\mathcal{H}} - \boldsymbol{S}\bar{\boldsymbol{d}})^T \boldsymbol{v}_1 + (\boldsymbol{S}\bar{\boldsymbol{d}} - \boldsymbol{d}^{\mathrm{L}}_{\mathcal{H}})^T \boldsymbol{v}_2 + Z(\tilde{\boldsymbol{f}}) - \sum_{(h,k,r)\in\mathcal{F}} \beta_{hkr} \tilde{f}_{hkr} \leq t \tag{27b}$$

$$\boldsymbol{D}^T \boldsymbol{u}_1 = \boldsymbol{y}_2 \tag{27c}$$

$$-\boldsymbol{D}^T \boldsymbol{u}_2 = \boldsymbol{y}_3 \tag{27d}$$

$$(\boldsymbol{S}\boldsymbol{D})^T \boldsymbol{v}_1 = \boldsymbol{y}_4 \tag{27e}$$

$$-(\boldsymbol{S}\boldsymbol{D})^T \boldsymbol{v}_2 = \boldsymbol{y}_5 \tag{27f}$$

$$\sum_{i=1}^{5} \boldsymbol{y}_i = (\boldsymbol{A}\boldsymbol{D})^T \boldsymbol{p} \tag{27g}$$

$$\boldsymbol{u}_1, \boldsymbol{u}_2, \boldsymbol{v}_1, \boldsymbol{v}_2 \geq 0 \tag{27h}$$

$$\text{Other constraints omitted} \tag{27i}$$

Eliminate t and put constraint 27b back to the objective function:

$$\hat{Z}(\boldsymbol{p})^{\mathrm{RC}} = \sum_{(h,k,r)\in\mathcal{F}} \beta_{hkr} \cdot (d_{hk} \cdot p_{hkr} - \tilde{f}_{hkr}) + \rho_{1-\varepsilon} \|\boldsymbol{y}_1\|_2 + (\boldsymbol{d}^{\mathrm{U}} - \bar{\boldsymbol{d}})^T \boldsymbol{u}_1 + (\bar{\boldsymbol{d}} - \boldsymbol{d}^{\mathrm{L}})^T \boldsymbol{u}_2$$
$$+ (\boldsymbol{d}^{\mathrm{U}}_{\mathcal{H}} - \boldsymbol{S}\bar{\boldsymbol{d}})^T \boldsymbol{v}_1 + (\boldsymbol{S}\bar{\boldsymbol{d}} - \boldsymbol{d}^{\mathrm{L}}_{\mathcal{H}})^T \boldsymbol{v}_2 + Z(\tilde{\boldsymbol{f}}) \tag{28}$$

which yields a second-order cone programming (SOCP).

Solution procedure

After incorporating the demand uncertainty, the final robust counterpart (RC) of the optimal flow problem can be formulated as:

$$[RC(\tilde{\boldsymbol{f}})] \quad \min_{\boldsymbol{p},\boldsymbol{u},\boldsymbol{v},\boldsymbol{y}} \quad \hat{Z}(\boldsymbol{p})^{\mathrm{RC}} = \sum_{(h,k,r)\in\mathcal{F}} \beta_{hkr}(\tilde{\boldsymbol{f}}) \cdot (d_{hk} \cdot p_{hkr} - \tilde{f}_{hkr}) + \rho_{1-\varepsilon} \|\boldsymbol{y}_1\|_2$$
$$+ (\boldsymbol{d}^{\mathrm{U}} - \bar{\boldsymbol{d}})^T \boldsymbol{u}_1 + (\bar{\boldsymbol{d}} - \boldsymbol{d}^{\mathrm{L}})^T \boldsymbol{u}_2 + (\boldsymbol{d}^{\mathrm{U}}_{\mathcal{H}} - \boldsymbol{S}\bar{\boldsymbol{d}})^T \boldsymbol{v}_1 + (\boldsymbol{S}\bar{\boldsymbol{d}} - \boldsymbol{d}^{\mathrm{L}}_{\mathcal{H}})^T \boldsymbol{v}_2 + Z(\tilde{\boldsymbol{f}}) \tag{29a}$$

$$\text{s.t.} \quad \text{Constraints } 27c - 27h \tag{29b}$$

$$\sum_{r\in R_k} p_{hkr} = 1 \quad \forall h \in \mathcal{H}, k \in \mathcal{K} \tag{29c}$$

$$0 \leq p_{hkr} \leq 1 \quad \forall (h,k,r) \in \mathcal{F} \tag{29d}$$

We observe that the ellipsoidal demand uncertainty performs like a regularization. It prevents p from being large in directions with considerable uncertainty in the demand. And this SOCP can be efficiently solved by inner interior point methods that are embedded in many existing solvers.

However, due to the first-order approximation of $Z(\boldsymbol{f})$, $\beta_{hkr}(\tilde{\boldsymbol{f}})$ need to be updated when a new flow pattern is obtained. Hence, after obtaining $\boldsymbol{p}^*$ from the RC problem, we need to run the simulation again to update $\beta_{hkr}(\tilde{\boldsymbol{f}})$. Before that, we need to get the corresponding worst-case demand (WD), which will be used as the new $\tilde{\boldsymbol{f}}$). It can be obtained by solving the worst case $\boldsymbol{z} \in \mathcal{Z}_{\text{E}} \cap \mathcal{Z}_{\text{P1}} \cap \mathcal{Z}_{\text{P2}}$:

$$[WD(\boldsymbol{p}^*)] \quad \max_{\boldsymbol{z}} \quad (\boldsymbol{A}\boldsymbol{D}\boldsymbol{z})^T \boldsymbol{p}^* \tag{30a}$$

$$\text{s.t.} \quad \|\boldsymbol{z}\|_2 \leq \rho_{1-\varepsilon} \tag{30b}$$

$$\boldsymbol{d}^{\text{L}} - \bar{\boldsymbol{d}} \leq \boldsymbol{D}\boldsymbol{z} \leq \boldsymbol{d}^{\text{U}} - \bar{\boldsymbol{d}} \tag{30c}$$

$$\boldsymbol{d}^{\text{L}}_{\mathcal{H}} - \boldsymbol{S}\bar{\boldsymbol{d}} \leq \boldsymbol{S}\boldsymbol{D}\boldsymbol{z} \leq \boldsymbol{d}^{\text{U}}_{\mathcal{H}} - \boldsymbol{S}\bar{\boldsymbol{d}} \tag{30d}$$

Denote the solution for Eq. 30 as $\boldsymbol{z}^*$. Then, the worse case demand is $\boldsymbol{d}^* = \bar{\boldsymbol{d}} + \boldsymbol{D}\boldsymbol{z}^*$. Next, we can update $\boldsymbol{\beta}(\tilde{\boldsymbol{f}})$ and $Z(\tilde{\boldsymbol{f}})$ as

$$Z(\tilde{\boldsymbol{f}}), \boldsymbol{\beta}(\tilde{\boldsymbol{f}}) = \text{Sim-FOA}(\boldsymbol{d}^*, \boldsymbol{p}^*) \tag{31}$$

where $\tilde{\boldsymbol{f}}$ in Eq. 31 indicates $\tilde{f}_{hkr} = d^*_{hk} \cdot p^*_{hkr}$. And Sim-FOA$(\cdot)$ is a pseudo function of simulation plus first-order approximation as described in Section 3.3. The RC, WD, and Sim-FOA$(\cdot)$ problems need to be solved iteratively. This can be treated as a fixed-point problem. A conventional way to solve a fixed-point problem is the method of successive average (MSA).

In the typical optimal **traffic** assignment problem, the optimal flow pattern is reached when for every OD pair, the marginal costs of all paths for this OD pair are the same. This implies that, ideally, when the flow distribution is optimal, we should have $\beta_{hkr}(\tilde{\boldsymbol{f}}) = \beta_{hkr'}(\tilde{\boldsymbol{f}})$ for all $r, r' \in R_k$. However, in our study, this cannot be set as the convergence criteria because in the dynamic **transit** assignment context, the cost function is not continuous due to left behind (i.e., adding one more passenger, the system travel time may be increased by one headway). And this may cause the criteria of $\beta_{hkr}(\tilde{\boldsymbol{f}}) = \beta_{hkr'}(\tilde{\boldsymbol{f}})$ never being satisfied. Therefore, in this study, we define the convergence criteria based on the value of system travel time: when the value of the system travel time is relatively stable within a range. Specifically, the MSA will converge if

$$\left| Z(\tilde{\boldsymbol{f}})^{(t)} - \frac{1}{T_c} \sum_{t'=t-T_c}^{t-1} Z(\tilde{\boldsymbol{f}})^{(t')} \right| \leq \epsilon \tag{32}$$

where $Z(\tilde{\boldsymbol{f}})^{(t)}$ is the system travel time at t-th iteration and ϵ is a predetermined threshold. Eq. 32 means that when the current system travel time is close to the average value of the last T_c iterations, the algorithm converge. Taking the average of the last T_c iterations can mitigate the impact of fluctuations caused by the discontinuity of the system travel time.

The whole solution algorithm is described in Algorithm 1. Line 6 indicates the MSA step. Lines 10 and 11 mean that we will use the path shares with the smallest system travel time over the last $T_c + 1$ iterations.

Let $\boldsymbol{p}^*$ be the optimal path shares solved from Algorithm 1. To realize the optimal path shares, the following system layouts can be used:

- Step 1: Transit operators deploy the recommendation system to smartphone apps, websites, and

Algorithm 1 Solution procedure of the robust optimal flow problem

Initialize $\boldsymbol{p}^{(0)}$, $\boldsymbol{d}^{(0)}$ and specify T_c, ϵ.
Set iteration counter $t = 0$.
do
  $Z(\tilde{\boldsymbol{f}})^{(t)}, \boldsymbol{\beta}(\tilde{\boldsymbol{f}})^{(t)} = \text{SIM-FOA}(\boldsymbol{d}^{(t)}, \boldsymbol{p}^{(t)})$
  Solve the RC problem (Eq. 29) with $Z(\tilde{\boldsymbol{f}})^{(t)}$ and $\boldsymbol{\beta}(\tilde{\boldsymbol{f}})^{(t)}$ as inputs, and return $\hat{\boldsymbol{p}}^{(t+1)}$
  $\boldsymbol{p}^{(t+1)} = \frac{1}{t+1}\hat{\boldsymbol{p}}^{(t+1)} + (1 - \frac{1}{t+1})\boldsymbol{p}^{(t)}$
  Solve the WD problem (Eq. 30) with $\boldsymbol{p}^{(t+1)}$ as input and return $\boldsymbol{d}^{(t+1)}$
  $t = t + 1$
while $t \leq T_c$ or $\left| Z(\tilde{\boldsymbol{f}})^{(t)} - \frac{1}{T_c} \sum_{t'=t-T_c}^{t-1} Z(\tilde{\boldsymbol{f}})^{(t')} \right| > \epsilon$
$t^* = \arg\min_{t'=t-T_c,\dots,t} Z(\tilde{\boldsymbol{f}})^{(t')}$
return $\boldsymbol{p}^{(t^*)}$

electrical screens at stations.

- Step 2: Passengers, when using the system, need to input their origins, destinations, and departure times.
- Step 3: For a passenger input OD pair k and departure time h, the system will return a single recommended path r to him/her with probability p^*_{hkr}.

EXTENSION TO ROLLING HORIZON

CASE STUDY DESIGN

In the case study, we consider an actual incident in the Blue line of the Chicago Transit Authority (CTA) urban rail system (Figure 3). The incident starts at 8:14 AM and ends at 9:13 AM on Feb 1st, 2019 due to infrastructures issues between Harlem and Jefferson Park stations. And the whole blue line is suspended. During the disruption, the destination for most of the passengers is the "Loop", which is the CBD area in Chicago. Usually, there are four paths leading to the Loop: 1) using blue line (i.e., waiting for the system to recovery), 2) using the parallel bus lines, 3) using the North-South (NS) bus lines to transfer to the Green line, and 4) using the West-East (WE) bus lines to transfer to Brown line. Based on the service structure, we can construct the route sets R_k for each OD pair k.

Parameter setting

$\mathcal{K}$ is set as all OD pairs with origins at the Blue line and destinations at the Loop. Time interval is set as $\tau = 10$ mins. The largest period with recommendation is $h_H = 10$, corresponding to 9:44 - 9:54 AM (i.e., 50 minutes after the end of the incident). In this study, we assume the incident duration is known. An alternative way to capture the incident duration uncertainty is stochastic optimization, that is, modeling the incident duration as multiple scenarios, and minimize the expectation of the system travel time.

Quantification of uncertainty sets

To quantify the demand uncertainty, we need to specify the nominal demand $\bar{\boldsymbol{d}}$, and covariance matrix $\boldsymbol{\Sigma}$ (which can be used to get $\boldsymbol{D}$), and upper and lower bounds for demand (i.e., $\boldsymbol{d}^{\mathrm{U}}$, $\boldsymbol{d}^{\mathrm{L}}$, $\boldsymbol{d}^{\mathrm{U}}_{\mathcal{H}}$, $\boldsymbol{d}^{\mathrm{L}}_{\mathcal{H}}$). These can be estimated from historical demand. However as the demand on the incident day

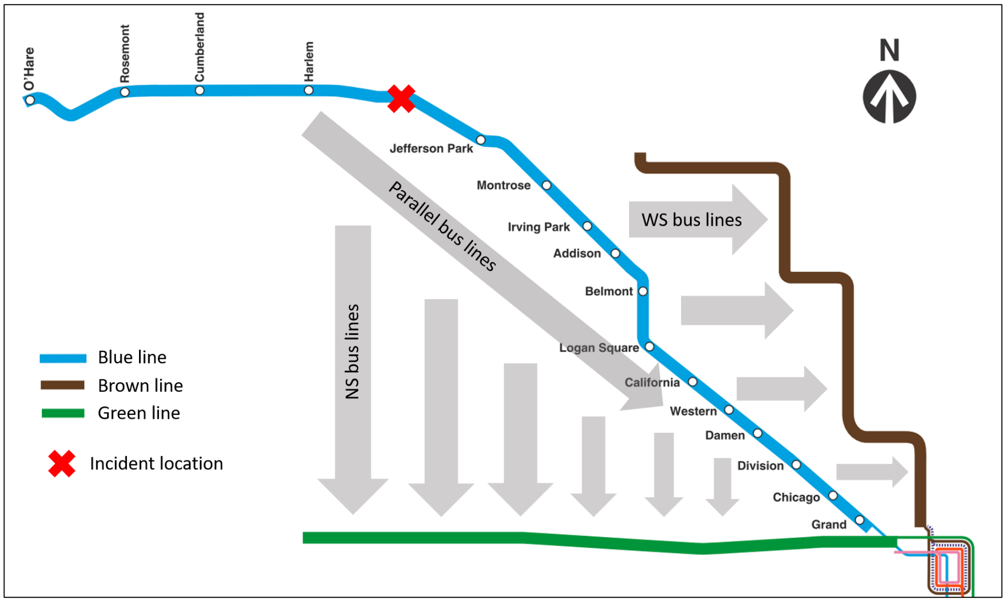

FIGURE 3: Case study diagram

is smaller than usual given some passengers may leave the system, we cannot directly use normal day smart card data as historical demand. One possible solution is to find previous days with similar incidents and use demand in those days as samples. But this is usually unavailable due to the lack of enough similar incidents. Hence, in this study, we first use survey results and historical smart card data to generate "synthetic historical demand" samples, and then estimate the uncertainty set from the samples.

Recall that the demand uncertainty comes from two parts: 1) the inherent demand variations across different days 2) and the uncertainty in how many passengers leaving the PT system during the incident. The first part can be captured by historical smart card data (without incidents). And the second part is approximated by the survey results. According to previous survey-based studies, the proportion of the number of passengers leaving the PT system during incidents is around 10%~30% (*26, 27*). The "synthetic historical demand" is generated as follows:

- Collect smart card data in a recent workday and calculate the demand vector without passengers leaving the system for each (h,k) (the demand for $h = 0$, i.e., offloading passengers, can be obtained using the simulation model).
- For each (h,k), randomly draw a proportion of leaving passengers from the uniform distribution $\mathcal{U}(0.1, 0.3)$. The demand after removing the leaving passengers is a sample demand vector.

We collected a total of 16 workdays from Jan 2019 (the previous month of the incident day) and generate 16 sample demand vectors. The mean value is used as the nominal demand $\bar{\boldsymbol{d}}$ and the co-variance matrix $\boldsymbol{\Sigma}$ are estimated from these samples. The upper and lower bounds for demand (i.e., $\boldsymbol{d}^{\mathrm{U}}$, $\boldsymbol{d}^{\mathrm{L}}$, $\boldsymbol{d}^{\mathrm{U}}_{\mathcal{H}}$, $\boldsymbol{d}^{\mathrm{L}}_{\mathcal{H}}$) are set as the samples' maximum and minimum values, respectively.

The hyperparameter $\rho_{1-\varepsilon}$ for the ellipsoidal uncertainty set are chosen from these values: $\{0, 0.25, 0.52, 0.84, 1.28, 1.64, 2.33\}$, which corresponds to $\{50, 60, 70, 80, 90, 95, 99\}$ percentiles of the standard norm distribution. Note that $\rho_{1-\varepsilon} = 0$ equals to no uncertainty (i.e., nominal model).

Data description

The nominal and actual (incident day) demands comparison are shown in Figure 4. The total nominal demand is 5,499, similar to the total actual demand (5,531), implying that introducing a proportion of leaving passengers (i.e., 10% - 30%) can capture the demand reduction in the incident day. We also observe that the aggregate nominal demand for each time interval is similar to that of the incident day. The major differences happen at the first two time intervals ($h = 0, 1$). However, looking at the disaggregate demand for each (h, k), the differences are more prominent. The discrepancy between nominal and actual demands provides potentials for the RO to perform better.

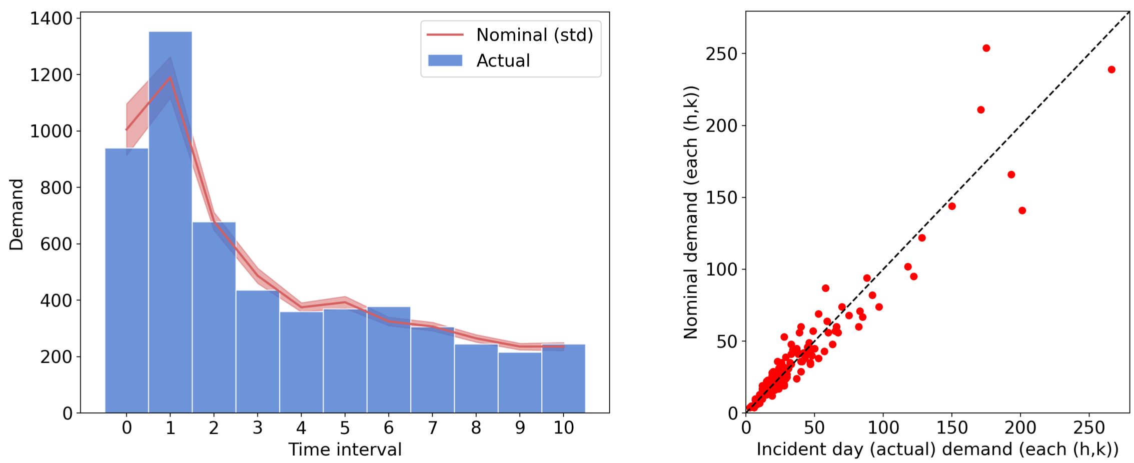

(a) Total demand for each time interval h

(b) Demand comparison for each (h, k)

FIGURE 4: Demand patterns

Table 1 shows the results of Mardia test of multivariate normality (*25*) for demand samples. The Mardia test is used to check whether the samples' multivariate skewness and kurtosis are consistent with a multivariate normal distribution. If both are satisfied, we can assume the samples are multivariate normally distributed. We observe that, in Table 1, the synthetic historical demands have consistent skewness but inconsistent kurtosis with the multivariate normal distribution, suggesting that they are not multivariate normally distributed. However, as skewness is a measure of the asymmetry of the probability distribution of a random variable about its mean, Mardia Skewness testing shows the demand distribution is symmetric. Hence, it is still reasonable to use the ellipsoidal uncertainty set to describe a symmetric distributed uncertain variable.

TABLE 1: Mardia test of multivariate normality

Test	p-value	Test	p-value
Mardia Skewness	1.00	Mardia Kurtosis	0.00

Note: Null hypothesis is that the samples are multivariate normally distributed.
The smaller p-value indicates we are more likely to reject the Null hypothesis.

Benchmark models

To compare with the optimization-based path recommendations, the following path shares are used as benchmarks.

Uniform path shares. The uniform path shares are defined as $p_{hkr} = \frac{1}{|R_k|} \; \forall \, r \in R_k$. This is a naive model corresponding to the intuition of "distributing passengers to different paths" when no information is available.

Capacity-based path shares. The capacity-based path shares aim to assign passengers to different paths according to the path capacity. Specifically, for a path in OD pair k and time h, we calculate the path capacity as the total available capacity of all vehicles passing through the first boarding station of the path. For example, for a path consisting of an NS bus route and the Green line, the path capacity is calculated as the total available capacity of all buses at the boarding station of the NS bus route during time interval h. The available capacity can be obtained from the simulation model using historical demand. The available capacity for the Blue line (i.e., incident line) depends on new operation schedules on the incident day (i.e., the service suspension is considered). When no vehicles operating in the Blue line, the path capacity will be zero.

Status-quo path shares. The status-quo path shares are the inferred path choices of passengers on the incident day. Since all passengers using WE, NS and parallel bus lines need to tap in, the demand increase (i.e., the number of incident day tap-ins minus the mean number of normal days tap-ins) in these lines can be seen as the number of passengers choosing the corresponding path. Hence, by identifying the demand increase for all nearby bus stops, we can get the number of passengers using the parallel bus, NS+Green, and WE+Brown paths for each OD pair k and time interval h. However, the number of waiting passengers in the Blue line is not directly recognizable because the CTA system does not record the tap-out information. Hence, we approximate the proportion of waiting passengers based on the survey results (*28*). Rahimi et al. (*28*) used a survival model to analyze the waiting time tolerance of CTA riders during a service disruption. The model results provide the proportion of waiting passengers given different system recovery times. Therefore, the status-quo path shares are inferred as follows.

- Step 1: Given the current time interval h and the incident end time T_e, obtain the remaining system recovery time if passengers choose to wait, based on which we can derive the proportion of waiting passengers using the results in (*28*).
- Step 2: For each OD pair k and time interval h, get the number of passengers using the parallel bus, NS+Green, and WE+Brown paths based on demand increase.
- Step 3: Fix the proportion of waiting passengers obtained from Step 1, other path shares are proportional to the number of passengers using the associated paths obtained in Step 2.

RESULTS

In this section, we demonstrate the model's performance in two steps. In the first step, we compare the optimization model without uncertainty (i.e., the nominal model with $\rho_{1-\epsilon} = 0$) with three benchmark path shares. This shows the improvement obtained from the optimization-based path recommendation. And in the second step, we compare the robust model with the nominal model, which shows the improvement from considering uncertainties.

Model convergence

Figure 5 shows the convergence of the nominal model ($\rho_{1-\epsilon} = 0$) and a robust model ($\rho_{1-\epsilon} = 0.84$). We observe that simulation-based linearization and MSA can successfully decrease the system travel time. And the model converges within 35 iterations. Note that the converged cost for the robust model is higher than the nominal model because the robust model is running with the worst-case demand (by definition with higher system travel time). The performance of all path recommendations will be evaluated on the actual demand (discussed in the next section).

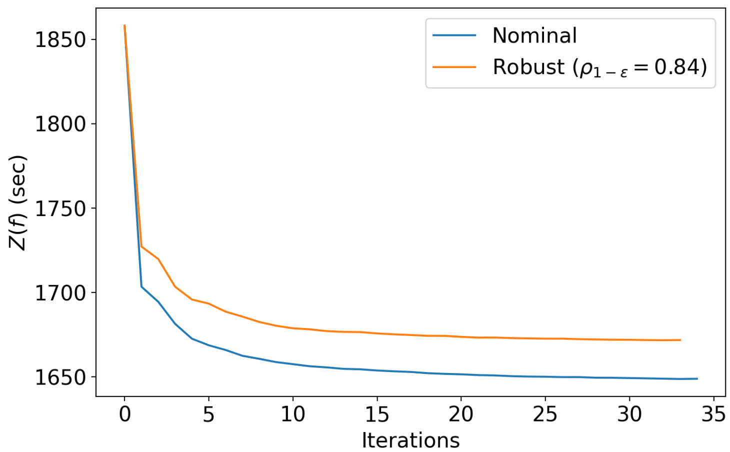

FIGURE 5: Convergence of optimization models

Model evaluation

The optimization model only utilizes the information of nominal demand and uncertainty set. The actual demand is unknown when running the model (otherwise there are no uncertainties). After obtaining the path shares (either from optimization or the benchmark models), the recommendation strategies will be evaluated based on the actual incident day demand using the simulation model. The model can output the travel time of every passenger in the system. And it can be used to compare the performances of different path shares.

Nominal model vs. Benchmark models

Table 2 compares the results of different path shares. The average travel times are calculated over all passengers (a total of 27,007 passengers) and the passengers who originally want to use the Blue line (i.e., passengers who are provided with recommendations, a total of 5,531 passengers). Results show that the optimization-based path shares can outperform all benchmark models. For all passengers in the system, the average travel time is reduced by 9.1% compared to the status quo. And for incident-line passengers, the reduction is even higher (20.6%).

We also observe that the uniform path shares are worse than the status quo scenario, meaning that current passengers' choices are not random and show some rationality. The capacity-based path shares can also significantly reduce the system travel time (by 6.9%). However, as the capacity-based path recommendations do not reflect the boarding order of upstream and downstream stations, it is worse than the optimization-based results.

Figure 6 shows the average travel time and waiting time for different paths. We observe that the optimization-based path shares have more evenly travel time across four types of paths, implying a better utilization of the system's capacity. However, for other path shares, passengers using parallel buses have significantly longer travel times than those using other paths. Looking

TABLE 2: Average travel time comparison

Path shares	All passengers (# 27,003)		Incident-line passengers (# 5,531)	
	Avg travel time (min)	% change[1]	Avg travel time (min)	% change
Uniform	31.02	+1.7%	54.64	+6.4%
Status quo	30.49	0%	51.34	0%
Capacity-based	28.36	-6.9%	43.23	-15.8%
Optimization (nominal)	27.71	**-9.1%**	40.75	**-20.6%**

[1]: changes compared to the status quo

at Figure 6, the average waiting time for the status quo scenario is around 30 minutes, which means most passengers chose to use the parallel bus during the incident, causing severe congestion. However, with the optimization-based path shares, the average waiting time for the parallel bus is less than 5 minutes (around a headway).

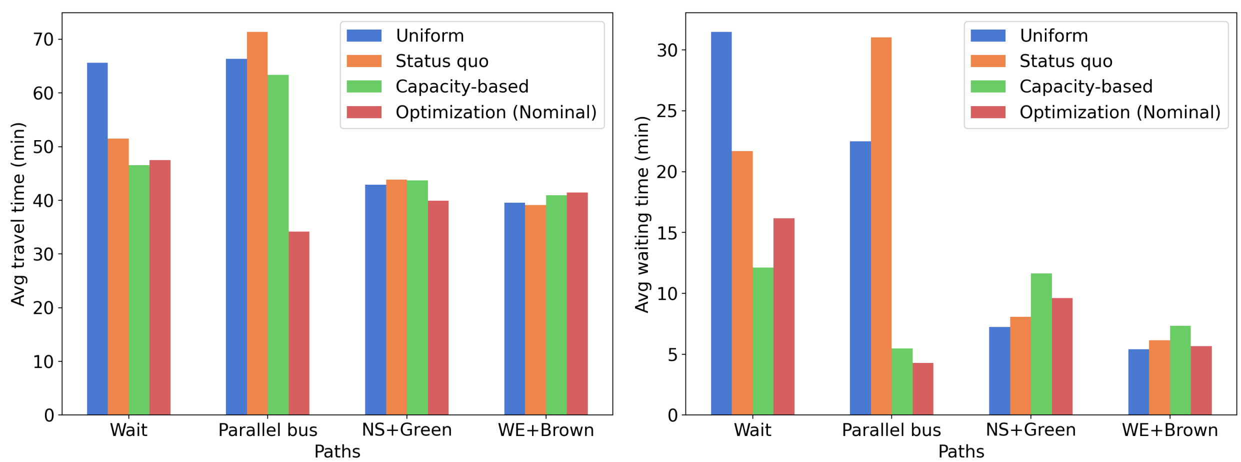

(a) Average travel time for different paths (b) Average waiting time for different paths

FIGURE 6: Comparison of average travel time and waiting time

The objective of this study is to minimize the system travel time. However, under the optimal path shares, some passengers' travel time may be increased compared to the status quo. Figure 7 shows the individual travel time change distribution (optimization-based minus the status quo) for all passengers with non-zero changes. We observe that, though most of the passengers have decreased travel time, some passengers become worse-off after following the path recommendation. This is a typical drawback of system optimal (first-best) assignment (*29*). Future studies may explore a Pareto-improving (second-best) path recommendation that ensuring no individual becomes worse-off.

Robust models vs. Nominal model

In this section, we compare the results of RO with different values of $\rho_{1-\epsilon}$. Figure 8 shows the average travel time of robust models. We observe that, except for $\rho_{1-\epsilon} = 2.33$, all other values show

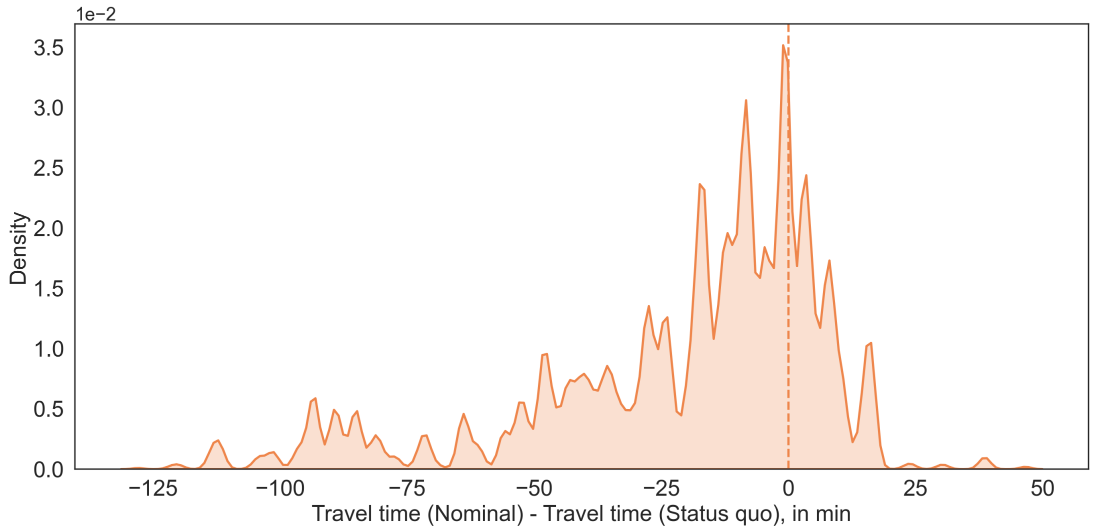

FIGURE 7: Distribution individual travel time changes

better performance than the nominal model. This implies that considering the demand uncertainty can further increase the path recommendation strategies. The best value is $\rho_{1-\epsilon} = 0.84$, where the travel time for incident line passengers is reduced by 2.91% compared to the nominal model. Note that the percentage decreases are relatively small because some passengers' travel times are not changed. If we only look at incident-line passengers with travel time changes, the average travel times are 47.6 min and 37.9 min for the nominal and RO ($\rho_{1-\epsilon} = 0.84$) scenarios, respectively, where the travel time reductions are 20.4%.

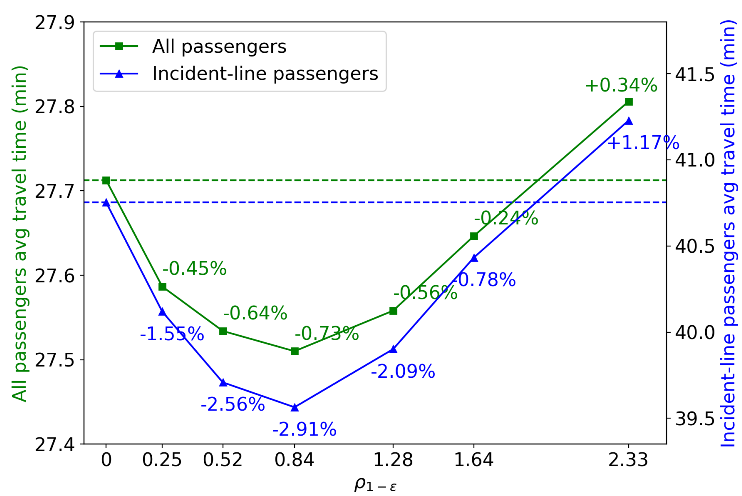

FIGURE 8: Performance of RO. The percentage changes are compared to the nominal scenario

Note that $\rho_{1-\epsilon} = 2.33$ indicates the largest uncertainty set compared to other values, under which the worst-case demand patterns may deviate from the actual demand too much, thus performs worse than the nominal model. To validate this, we plot the worst-case demand for different values of $\rho_{1-\epsilon}$ in Figure 9. It is found that the worst-case demands for $\rho_{1-\epsilon} = 0.52, 0.84, 1.28$ scenarios are closer to the actual demand, and $\rho_{1-\epsilon} = 2.33$ overestimate the demands for $h = 0, 1$. These results are consistent with the travel time performance in Figure 8.

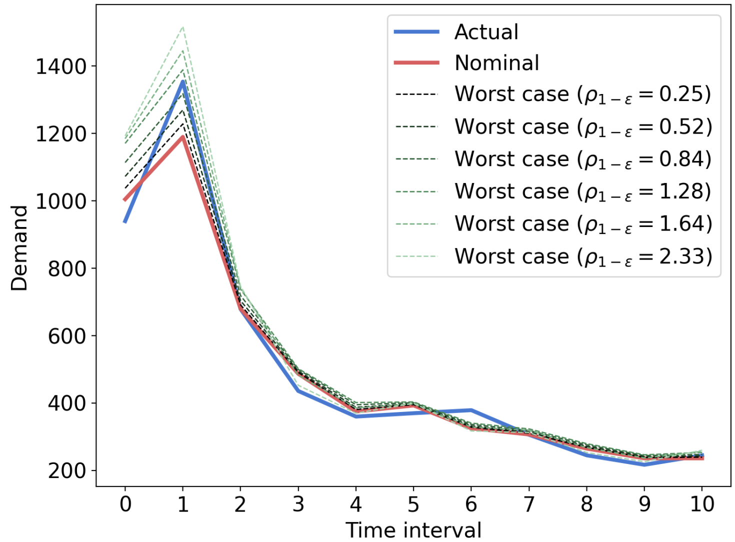

FIGURE 9: Worst-case demand patterns

CONCLUSION AND DISCUSSION

In this paper, we propose a path recommendation model to mitigate the congestion during public transit disruptions. Passengers with different ODs and departure times are recommended with different paths such that the system travel time is minimized. To tackle the non-analytical formulation of travel times due to left behind, we propose a simulation-based first-order approximation to transform the original problem into linear programming. Uncertainties in demand are modeled with RO techniques to protect the path recommendation strategies against inaccurate estimates. A real-world rail disruption scenario in the CTA system is used as a case study. Results show that even without considering uncertainty, the nominal model can reduce the system travel time by 9.1% (compared to status quo), and outperforms the benchmark capacity-based path recommendation. After incorporating the demand uncertainty, the robust model can further reduce the system travel time. The best robust model with $\rho_{1-\epsilon} = 0.84$ can decrease the average travel time of incident-line passengers by 2.91% compared to the nominal model.

AUTHOR'S CONTRIBUTION

The authors confirm contribution to the paper as follows: study conception and design: B. Mo, H.N. Koutsopoulos, J. Zhao; data collection: B. Mo; analysis and interpretation of results: B. Mo; draft manuscript preparation: B. Mo. All authors reviewed the results and approved the final version of the manuscript.

ACKNOWLEDGEMENT

The authors would like to thank Chicago Transit Authority (CTA) for their support and data availability for this research.

REFERENCES

1. Cox, A., F. Prager, and A. Rose, Transportation security and the role of resilience: A foundation for operational metrics. *Transport policy*, Vol. 18, No. 2, 2011, pp. 307–317.
2. Mo, B., M. Y. v. Franque, H. N. Koutsopoulos, and J. Zhao, Impact of Unplanned Rail Disruption on Urban Transit Systems. In *Transportation Rsearch Board 100th Annual Meeting*, 2021.
3. De Cea, J. and E. Fernández, Transit assignment for congested public transport systems: an equilibrium model. *Transportation science*, Vol. 27, No. 2, 1993, pp. 133–147.
4. Bruglieri, M., F. Bruschi, A. Colorni, A. Luè, R. Nocerino, and V. Rana, A real-time information system for public transport in case of delays and service disruptions. *Transportation Research Procedia*, Vol. 10, 2015, pp. 493–502.
5. Böhmová, K., M. Mihalák, T. Pröger, R. Srámek, and P. Widmayer, Robust routing in urban public transportation: How to find reliable journeys based on past observations. In *ATMOS-13th Workshop on Algorithmic Approaches for Transportation Modelling, Optimization, and Systems-2013*, Schloss Dagstuhl—Leibniz-Zentrum fuer Informatik, 2013, Vol. 33, pp. 27–41.
6. Roelofsen, D., O. Cats, N. van Oort, and S. Hoogendoorn, Assessing disruption management strategies in rail-bound urban public transport systems from a passenger perspective. In *Proceedings of the 14th Conference on Advanced Systems in Public Transport (CASPT), Brisbane, Australia*, 2018.
7. Wu, J. H., M. Florian, and P. Marcotte, Transit equilibrium assignment: a model and solution algorithms. *Transportation Science*, Vol. 28, No. 3, 1994, pp. 193–203.
8. Schmöcker, J.-D., A. Fonzone, H. Shimamoto, F. Kurauchi, and M. G. Bell, Frequency-based transit assignment considering seat capacities. *Transportation Research Part B: Methodological*, Vol. 45, No. 2, 2011, pp. 392–408.
9. Nielsen, O. A., A stochastic transit assignment model considering differences in passengers utility functions. *Transportation Research Part B: Methodological*, Vol. 34, No. 5, 2000, pp. 377–402.
10. Nguyen, S., S. Pallottino, and F. Malucelli, A modeling framework for passenger assignment on a transport network with timetables. *Transportation Science*, Vol. 35, No. 3, 2001, pp. 238–249.
11. Hamdouch, Y. and S. Lawphongpanich, Schedule-based transit assignment model with travel strategies and capacity constraints. *Transportation Research Part B: Methodological*, Vol. 42, No. 7-8, 2008, pp. 663–684.
12. Hamdouch, Y., W. Szeto, and Y. Jiang, A new schedule-based transit assignment model with travel strategies and supply uncertainties. *Transportation Research Part B: Methodological*, Vol. 67, 2014, pp. 35–67.
13. Schmöcker, J.-D., M. G. Bell, and F. Kurauchi, A quasi-dynamic capacity constrained frequency-based transit assignment model. *Transportation Research Part B: Methodological*, Vol. 42, No. 10, 2008, pp. 925–945.
14. Ben-Tal, A., L. El Ghaoui, and A. Nemirovski, *Robust Optimization*. Princeton Series in Applied Mathematics, Princeton University Press, 2009.
15. Bertsimas, D., D. B. Brown, and C. Caramanis, Theory and applications of robust optimization. *SIAM Review*, Vol. 53, No. 3, 2011, pp. 464–501.

16. Ben-Tal, A. and A. Nemirovski, Robust convex optimization. *Mathematics of Operations Research*, Vol. 23, No. 4, 1998, pp. 769–805.
17. Ben-Tal, A. and A. Nemirovski, Robust solutions of uncertain linear programs. *Operations Research Letters*, Vol. 25, No. 1, 1999, pp. 1–13.
18. Bertsimas, D. and M. Sim, The price of robustness. *Operations Research*, Vol. 52, No. 1, 2004, pp. 35–53.
19. Xiong, P., P. Jirutitijaroen, and C. Singh, A distributionally robust optimization model for unit commitment considering uncertain wind power generation. *IEEE Transactions on Power Systems*, Vol. 32, No. 1, 2016, pp. 39–49.
20. Ma, C., W. Hao, R. He, X. Jia, F. Pan, J. Fan, and R. Xiong, Distribution path robust optimization of electric vehicle with multiple distribution centers. *PloS One*, Vol. 13, No. 3, 2018.
21. Wang, Y., Y. Zhang, and J. Tang, A distributionally robust optimization approach for surgery block allocation. *European Journal of Operational Research*, Vol. 273, No. 2, 2019, pp. 740–753.
22. Guo, X., N. S. Caros, and J. Zhao, Robust matching-integrated vehicle rebalancing in ride-hailing system with uncertain demand. *Transportation Research Part B: Methodological*, Vol. 150, 2021, pp. 161–189.
23. Mo, B., Z. Ma, H. N. Koutsopoulos, and J. Zhao, Capacity-constrained network performance model for urban rail systems. *Transportation Research Record*, 2020, p. 0361198120914309.
24. Bertsimas, D. and D. den Hertog, *Robust and adaptive optimization*. Dynamic Ideas LLC, Belmont, Massachusetts, 2020.
25. Cain, M. K., Z. Zhang, and K.-H. Yuan, Univariate and multivariate skewness and kurtosis for measuring nonnormality: Prevalence, influence and estimation. *Behavior research methods*, Vol. 49, No. 5, 2017, pp. 1716–1735.
26. Lin, T., A. Shalaby, and E. Miller, Transit User Behaviour in Response to Service Disruption: State of Knowledge. In *Canadian Transportation Research Forum 51st Annual Conference-North American Transport Challenges in an Era of Change//Les défis des transports en Amérique du Nord à une aire de changement Toronto, Ontario*, 2016.
27. Rahimi, E., A. Shamshiripour, R. Shabanpour, A. Mohammadian, and J. Auld, Analysis of Transit Users' Response Behavior in Case of Unplanned Service Disruptions. *Transportation Research Record*, 2020, p. 0361198120911921.
28. Rahimi, E., A. Shamshiripour, R. Shabanpour, A. Mohammadian, and J. Auld, Analysis of transit users' waiting tolerance in response to unplanned service disruptions. *Transportation Research Part D: Transport and Environment*, Vol. 77, 2019, pp. 639–653.
29. Lawphongpanich, S. and Y. Yin, Solving the Pareto-improving toll problem via manifold suboptimization. *Transportation Research Part C: Emerging Technologies*, Vol. 18, No. 2, 2010, pp. 234–246.